



## Pharmaceutical nanotechnology

Development of andrographolide loaded PLGA microspheres: Optimization, characterization and *in vitro*–*in vivo* correlationYunxia Jiang, Fang Wang, Hui Xu<sup>\*</sup>, Hui Liu, Qingguo Meng, Wanhui Liu

School of Pharmacy, Yantai University, Yantai 264005, China

## ARTICLE INFO

## Article history:

Received 25 May 2014

Received in revised form 23 August 2014

Accepted 10 September 2014

Available online 16 September 2014

## Keywords:

Andrographolide

PLGA

Microspheres

RSM

Drug release

*In vitro*–*in vivo* correlation

## ABSTRACT

The purpose of this study was to develop a sustained-release drug delivery system based on the injectable PLGA microspheres loaded with andrographolide. The andrographolide loaded PLGA microspheres were prepared by emulsion solvent evaporation method with optimization of formulation using response surface methodology (RSM). Physicochemical characterization, *in vitro* release behavior and *in vivo* pharmacokinetics of the optimized formulation were then evaluated. The percent absorbed *in vivo* was determined by deconvolution using the Loo–Riegelman method, and then the *in vitro*–*in vivo* correlation (IVIVC) was established. Results showed that the microspheres were spherical with a smooth surface. Average particle size, entrapment efficiency and drug loading were found to be  $53.18 \pm 2.11 \mu\text{m}$ ,  $75.79 \pm 3.02\%$  and  $47.06 \pm 2.18\%$ , respectively. *In vitro* release study showed a low initial burst release followed by a prolonged release up to 9 days and the release kinetics followed the Korsmeyer–Peppas model. After a single intramuscular injection, the microspheres maintained relatively high plasma concentration of andrographolide over one week. A good linear relationship was observed between the *in vitro* and *in vivo* release behavior ( $R^2 = 0.9951$ ). These results suggest the PLGA microspheres could be developed as a potential delivery system for andrographolide with high drug loading capacity and sustained drug release.

© 2014 Elsevier B.V. All rights reserved.

## 1. Introduction

Since the era of chemotherapy began in 1940s with the first use of nitrogen mustards and antifolate drugs, cancer drug discovery and development have been the major research endeavor around the globe (Efferth et al., 2007). The compounds that inhibit multiple precancer events are of great interest as they are more likely to prevent a wide range of cancers under a great variety of circumstances (Akbar, 2011; Boik, 2001). Naturally occurring drugs are therefore among the major players against cancer, and almost half of all the anti-cancer drugs used today are either natural products or their derivatives, including taxanes, vinca alkaloids, anthracyclines and derivatives of podophyllotoxin and camptothecin (Cragg and Newman, 2005; Newman and Cragg, 2012).

*Andrographis paniculata* (Burm. F.) Wall. Ex. Nees. is a herbaceous medicinal plant native to China, India and other southeast Asian countries. It belongs to the family Acanthaceae and is commonly known as “Kalmegh or King of Bitters” for the bitter taste of all parts of the plant (Sudhakaran, 2012). The aerial part of

*A. paniculata* has been widely used in Chinese medicine as a heat-clearing and detoxifying agent to get rid of internal body heat, inflammation and pain. It is also used to dispose of toxins from body and as a remedy for common cold, dysentery, fever, tonsillitis, diarrhea, liver diseases and herpes since ancient times (Deng, 1978; Mandal et al., 2001; Tang and Eisenbrand, 1992). Diterpenoid lactone andrographolide (AG) is one of the principal constituents of *A. paniculata*, and has proven to be mainly responsible for the therapeutic properties of this herbal medicine (Maiti et al., 2006). What is fascinating is that AG could act both directly and indirectly on cancer cells and exhibit strong potential as a potent anti-cancer agent, which involves inhibiting proliferation, induction of apoptosis and cell-cycle arrest, immunostimulating properties, anti-angiogenic and chemo-protective activities (Kumar et al., 2004; Rajagopal et al., 2003; Varma et al., 2011; Vojdani and Erde, 2006). However, formulation development of AG has been limited by its unsatisfactory physicochemical and ADME properties, which include very poor aqueous solubility, instability in extreme acidic or alkaline conditions of the gastrointestinal tract (Chellampillai and Pawar, 2011; Panossian et al., 2000), as well as poor oral absorption and low bioavailability due to rapid and extensive metabolism and efflux by P-glycoprotein (Gu et al., 2007; Ye et al., 2011). Furthermore, it has been reported that intravenous

<sup>\*</sup> Corresponding author. Tel.: +86 535 6706030; fax: +86 535 6706066.  
E-mail addresses: [yutu309a@163.com](mailto:yutu309a@163.com), [xuhui33@sina.com](mailto:xuhui33@sina.com) (H. Xu).

administration of large dosage of AG within a short time may induce nephrotoxicity (Hu et al., 2009; Lu et al., 2010). It therefore continues to be highlighted as a major challenge to develop effective drug delivery systems of AG for potential chemotherapeutic use, although several strategies such as complexation with cyclodextrine, preparation of liposome, solid dispersion and nanoparticles have been attempted to improve aqueous solubility and *in vivo* circulation time of this compound (Bothiraja et al., 2009; Roy et al., 2009; Sinha et al., 2000; Zhao et al., 2002).

Microsphere is an innovative approach with many advantages to overcome formulation defects as well as adverse effects of anticancer compounds (Barrow, 2004; Sinha and Trehan, 2005). Controlled-release microsphere formulation can be topically administered by implantation, intratumoral injection, or transcatheter arterial chemoembolization, and have the potential to selectively increase tumor exposure to drugs with little systemic toxicity (Benoit et al., 2000; Liu et al., 2003). Over the past two decades, microspheres thus have been developed as potential formulation and widely applied in cancer treatment, such as polyvinyl alcohol microspheres loaded with doxorubicin and gelatin microspheres loaded with cisplatin (Cheung et al., 2005; Toyama et al., 2012; Ventura et al., 2011; Wang et al., 1996). However, AG loaded microsphere formulation for cancer therapy has not been reported yet.

With poly (D,L-lactide-co-glycolide) (PLGA) as drug carrier, the present study aimed to develop an AG loaded microsphere formulation with a sustained release of AG as a potential anticancer agent. A solid-in-oil-in-water (s/o/w) emulsion solvent evaporation technique was used to prepare the AG loaded PLGA microspheres, and RSM was applied for formulation optimization. Physicochemical characterization, *in vitro* release behavior and *in vivo* pharmacokinetics of the optimized formulation were then investigated.

## 2. Materials and methods

### 2.1. Materials and reagents

Andrographolide (AG) was obtained from Sichuan Huakang Pharmaceutical Raw Material Factory (Shifang, China). Poly (D,L-lactide-co-glycolide) (PLGA, lactide/glycolide ratio 50:50, inherent viscosity 0.20 dL/g, Mw 18 kDa) was produced by Shandong Luye Pharmaceutical Co., Ltd. (Yantai, China). Poly vinyl alcohol (PVA, Mw 13,000–23,000) was purchased from Sigma-Aldrich (St. Louis, Missouri, USA). Dehydroandrographolide was used as an internal standard (IS) for quantification and purchased from National Institute for the Control of Pharmaceutical and Biological Products (Beijing, China). Methanol was of HPLC grade and obtained from Oceanpak Alexative Chemical (Gothenburg, Sweden). Deionized water produced by Wahaha Co., Ltd., (Hangzhou, China) was used throughout the study. All other chemicals and solvents used were purchased from Sinopharm Chemical Reagent Co., Ltd., (Shanghai, China) and at least of analytical grade.

### 2.2. Preparation of the microspheres

Briefly, a specified amount of PLGA was dissolved in 2.5 mL of methylene chloride, and 0.5 g of amorphous AG fine powder with a mean particle size of 0.5  $\mu\text{m}$  was dispersed in the polymer solution under sonication (JY92-II, Ningbo, China) for 30 s in an ice-water bath. Then a drug polymer suspension was obtained and added dropwise to a specified volume of aqueous solution containing PVA under magnetic stirring at 1000 rpm for 3 min. In order to allow the microspheres solidification, a slower stirring at 600 rpm was continued for 4 h until the methylene chloride

completely evaporated. After centrifugation at 3000 rpm for 3 min (TGL-20 M, Changsha, China), the microspheres were collected and then washed three times with distilled water in order to remove traces of the residual solvent and PVA. The resulting microspheres were finally freeze-dried and then stored at 4 °C for further evaluation.

### 2.3. Experimental design

The Box–Behnken design (BBD) is suitable for investigating the quadratic response surfaces and for constructing second-order polynomial models using Design-Expert® (Version 8.0.7.1, State-Ease Inc., Minneapolis, MN, USA), thus enabling optimization of a process with a small number of experimental runs (Yang et al., 2010). In this work, a three-factor, three-level BBD was employed to optimize the formulation parameters of microsphere preparation on the basis of preliminary study. The PLGA concentration ( $X_1$ ), PVA concentration ( $X_2$ ) and the organic phase/aqueous phase (o/w) volume ratio ( $X_3$ ) were selected as three independent variables, while the particle size ( $Y_1$ ) and entrapment efficiency ( $Y_2$ ) were dependent variables. The independent variables selected are shown in Table 1 along with their low, medium and high levels, which were determined from preliminary trials. The design matrix was generated by the software and consisted of 17 experimental runs including 12 factorial points at the midpoints of the edges of the process space and 5 replicates at the center point for estimation of pure error sum of squares, shown in Table 2. To avoid bias, all the experiments were performed in random order.

The non-linear quadratic model generated by the design was:

$$Y = b_0 + b_1X_1 + b_2X_2 + b_3X_3 + b_4X_1X_2 + b_5X_1X_3 + b_6X_2X_3 + b_7X_1^2 + b_8X_2^2 + b_9X_3^2 \quad (1)$$

in which  $Y$  is the measured response associated with each factor level combination;  $b_0$  is an intercept;  $b_1$ – $b_9$  are the regression coefficients computed from the observed experimental values of  $Y$ ;  $X_1$ ,  $X_2$  and  $X_3$  are the coded levels of independent variables. The terms  $X_iX_j$  and  $X_i^2$  ( $i=1, 2$  or  $3$ ) represent the interaction and quadratic terms, respectively (Gannu et al., 2010). Design-Expert software was used to perform the statistical data analysis of the regression model and plot the response surface graphs.

### 2.4. Characterization of the microspheres

#### 2.4.1. Morphological characterization and particle sizing

The surface morphology of the PLGA microspheres was observed using a JEOL JSM-5610LV scanning electron microscope (JEOL, Tokyo, Japan). The lyophilized microspheres were mounted on metal stubs with an adhesive carbon tape, sputter-coated with gold and examined under the microscope at an acceleration voltage of 15 kV.

The average particle size and size distribution of the PLGA microspheres were measured by Malvern 2000 laser particle size analyzer (Malvern Instruments Ltd., Malvern, UK). For this analysis, the lyophilized microspheres were suspended in distilled water. The polydispersity index (PDI) was calculated to evaluate the size distribution. The PDI usually ranges from 0.1 to 0.5 and the lower value of PDI means better homogeneity in size distribution.

**Table 1**

The independent variables and their levels in the Box–Behnken design.

Independent variables	Levels		
	Low (−1)	Medium (0)	High (+1)
$X_1$ = PLGA concentration (% w/v)	10	15	20
$X_2$ = PVA concentration (% w/v)	0.5	1.25	2
$X_3$ = o/w ratio (v/v)	0.01	0.015	0.02

**Table 2**

Box–Behnken experimental design and the observed responses.

Run	Independent variables			Dependent variables	
	PLGA concentration ( $X_1$ , % w/v)	PVA concentration ( $X_2$ , % w/v)	o/w ratio ( $X_3$ , v/v)	Particle size ( $Y_1$ , $\mu\text{m}$ )	Entrapment efficiency ( $Y_2$ , %)
1	15	2	0.02	68.56	42.44
2	20	1.25	0.01	55.66	49.97
3	10	1.25	0.02	42.86	24.99
4	20	1.25	0.02	66.87	48.36
5	15	0.5	0.02	108.29	77.49
6	15	2	0.01	61.21	51.79
7	20	2	0.015	65.62	39.98
8	15	1.25	0.015	52.51	69.57
9	10	1.25	0.01	37.11	36.15
10	20	0.5	0.015	114.57	70.52
11	10	0.5	0.015	81.96	59.14
12	15	0.5	0.01	115.09	90.77
13	15	1.25	0.015	51.36	68.09
14	15	1.25	0.015	50.94	67.51
15	15	1.25	0.015	46.54	66.61
16	15	1.25	0.015	46.33	65.65
17	10	2	0.015	51.35	21.72

#### 2.4.2. Drug loading and entrapment efficiency

The amount of AG encapsulated in the PLGA microspheres was determined by HPLC method. Briefly, accurately weighed 10 mg of AG loaded PLGA microspheres were dissolved in 10 mL of methylene chloride followed by a 10-fold dilution with the mobile phase consisting of methanol–water (55:45, v/v). After centrifugation at 5000 rpm for 10 min, the supernatant was collected and injected into an Agilent 1100HPLC system (Agilent Technologies, Santa Clara, USA) to determine the concentration of AG. The determination was performed on a Diamonsil C18 column (150 mm  $\times$  4.6 mm, 5  $\mu\text{m}$ , Dikma Technologies, USA) with the column temperature maintained at 30 °C. The mobile phase was delivered at a flow rate of 1 mL/min. The detection wavelength was set at 225 nm and the injection volume was 20  $\mu\text{L}$ . All measurements were conducted in triplicate and the results were expressed as mean  $\pm$  SD.

The drug loading (%) and entrapment efficiency (%) were calculated by the following equations, respectively.

$$\text{Drug loading}(\%) = \frac{\text{amount of drug in microspheres}}{\text{amount of microspheres}} \times 100 \quad (2)$$

$$\text{Entrapment efficiency}(\%) = \frac{\text{amount of drug in microspheres}}{\text{theoretical amount of drug}} \times 100 \quad (3)$$

where the theoretical amount of drug refers to the initial amount of drug used for the preparation of microspheres.

#### 2.5. Residual solvent analysis

The residual level of methylene chloride in the microspheres was determined by an Agilent 6890N gas chromatograph (GC) equipped with a flame ionized detector (FID) and a DB-624 capillary column (30 m  $\times$  0.32 mm, 1.8  $\mu\text{m}$ ). Nitrogen was used as carrier gas and the flow of carrier was 1.0 mL/min. The split injection mode was used with a split ratio of 10:1. The initial column temperature was 40 °C maintained for 3 min and then raised (10 °C/min) to 210 °C for 5 min. The temperature of injection port and detector was 230 °C and 240 °C, respectively. Dimethylsulfoxide (DMSO) was used as solvent to dissolve the microspheres, and 1  $\mu\text{L}$  of this solution was injected into the GC for analysis. The calibration curve showed good linearity over the

concentration range of 1.0–10  $\mu\text{g/mL}$  and the recovery was between 98.53% and 99.32% with RSD less than 1.0%.

#### 2.6. In vitro release study

The *in vitro* release profile of AG from PLGA microspheres was determined as follows. Briefly, 50 mg of AG loaded PLGA microspheres were suspended in 30 mL of phosphate buffered saline (PBS, pH 7.4, 0.05 M) containing 0.02% Tween-80 and 0.05% SDS (sodium dodecyl sulfate). The microsphere suspension was shaken horizontally at 70 rpm in a shaking water bath maintained at 37 °C (HZS-HA, Haerbin, China). At predetermined time intervals, the samples were centrifuged at 5000 rpm for 10 min before the supernatant was withdrawn and the sediment of microspheres was re-dispersed in an equal amount of fresh PBS. The supernatant collected was filtered through a 0.45  $\mu\text{m}$  filter (MillexGV, Millipore, USA) and the AG concentration in the filtrate was determined by the HPLC method as described above. All measurements were conducted in triplicate and the results were expressed as the mean  $\pm$  SD.

In order to investigate the mechanism of AG release from PLGA microspheres, the *in vitro* release data was analyzed by the following kinetic models including zero order (Eq. (4)), first order (Eq. (5)), Higuchi (1963) (Eq. (6)) and Korsmeyer–Peppas (Korsmeyer et al., 1983; Peppas, 1985) (Eq. (7)) equations.

$$Q_t = k_0 t \quad (4)$$

$$\ln(1 - Q_t) = -k_1 t \quad (5)$$

$$Q_t = k_H t^{1/2} \quad (6)$$

$$\ln Q_t = n \ln t + k \quad (7)$$

where  $Q_t$  is the cumulative percentage of drug release at time  $t$ ,  $k$  is the release rate constant,  $n$  is the release exponent indicative of mechanism of drug release. Regression analysis was performed and the coefficient of determination ( $R^2$ ) was calculated to evaluate the kinetic models. The model which gave the highest value of  $R^2$  was considered to be the most suitable kinetic model for describing the release of AG from the PLGA microspheres.

## 2.7. In vivo pharmacokinetic study

### 2.7.1. Animals and drug administration

Healthy male Sprague-Dawley (SD) rats weighing  $220 \pm 20$  g were supplied by the Experimental Animal Center of Shandong Luye Pharmaceutical Co., Ltd. (Yantai, China). All rats were acclimatized in animal house for one week and were fed with standard diet and water *ad libitum*. The rats were fasted overnight before the drug administration but with free access to water throughout the study. The study conformed to the Guide for the Care and Use of Laboratory Animals.

Twelve rats were randomly divided into two groups with 6 rats each. Group I received pure AG solution dissolved in DMSO at a single dose of 2 mg/kg by intravenous (i.v.) injection. The blood samples were obtained via the orbital venous plexus and collected into heparinized tubes immediately prior to dosing and at 0.083, 0.167, 0.333, 0.5, 1, 2, 3, 4, 6, 8, 12, and 24 h after dosing. Group II received AG loaded microspheres suspension in water at a single dose of 10 mg/kg by intramuscular (i.m.) injection. The blood samples were collected into heparinized tubes immediately prior to dosing and at 1, 2, 4, 8, 12 h, and 1–10 days after dosing. All the blood samples were centrifuged immediately at 6000 rpm for 5 min and the plasma samples were then obtained and stored at  $-20^\circ\text{C}$  until analysis.

### 2.7.2. Sample preparation and quantification

The AG concentration in plasma was determined by LC–MS/MS analysis according to the method reported (Xu et al., 2009) with slight modifications. After thawing at room temperature, an aliquot of 100  $\mu\text{L}$  plasma sample was spiked with 20  $\mu\text{L}$  of IS working solution (500 ng/mL) and mixed for 30 s. After the addition of 300  $\mu\text{L}$  of methanol, the mixture was vortex mixed for 5 min and then centrifuged at 12,000 rpm for 10 min. A 10  $\mu\text{L}$  aliquot of the supernatant was injected into the HPLC–ESI–MS/MS system for analysis.

A TSQ Quantum Access triple-quadrupole tandem mass spectrometer (Thermo Fisher Scientific Inc., Waltham, MA, USA) was connected to Agilent 1100HPLC system (Agilent Technologies, Santa Clara, USA) via electro-spray ionization (ESI) interface. LC–MS/MS was carried out using nitrogen to assist nebulization, and Xcalibur software version 1.4 was used for system control and data processing. LC separation was performed on a Luna C18 column (150 mm  $\times$  4.6 mm, 5  $\mu\text{m}$ , Phenomenex) with a mobile phase of methanol–water (70:30, v/v) at a flow rate of 0.5 mL/min at  $30^\circ\text{C}$ . The mass spectrometer was operated in the negative ion mode and selective ion monitors (SIM) were at  $m/z$  331 ( $[\text{M}-\text{H}_2\text{O}-\text{H}]^-$ ) for AG and 331 ( $[\text{M}-\text{H}]^-$ ) for IS, respectively. Ultra-high purity helium was used as the damping and collision gas, and nitrogen as the sheath and auxiliary gas. The main parameters were optimized as follows: sheath gas 30 psi and 0.75 L/min, auxiliary gas 10 psi and 0.15 L/min, collision gas 1.5 mTorr and 0.75 L/min, electrospray needle voltage 4.5 kV, capillary voltage 30 V, and heated capillary temperature  $350^\circ\text{C}$ .

**Table 3**

Summary of results of regression analysis for responses  $Y_1$  and  $Y_2$ .

Models	$R^2$	Adjusted $R^2$	Predicted $R^2$	SD	Adequate precision	%CV	Remark
Particle size ( $Y_1$ )							
Linear	0.4825	0.3631	0.0469	19.87	–	–	–
Second order	0.4968	0.1948	–1.0444	22.34	–	–	–
Quadratic	0.9905	0.9783	0.8968	3.67	27.434	5.58	Suggested
Entrapment efficiency ( $Y_2$ )							
Linear	0.5732	0.4747	0.2223	13.61	–	–	–
Second order	0.5801	0.3281	–0.6767	15.39	–	–	–
Quadratic	0.9942	0.9867	0.9298	2.16	41.461	3.87	Suggested

**Table 4**

Coefficients of the quadratic models and their corresponding  $p$ -values<sup>a</sup>.

Factor	Particles size ( $Y_1$ )		Entrapment efficiency ( $Y_2$ )	
	Coefficient	$p$ -value	Coefficient	$p$ -value
Intercept	49.54		67.49	
$X_1$	11.18	<b>&lt;0.0001</b>	8.35	<b>&lt;0.0001</b>
$X_2$	–21.65	<b>&lt;0.0001</b>	–17.75	<b>&lt;0.0001</b>
$X_3$	2.19	0.1350	–4.43	<b>0.0007</b>
$X_1X_2$	–4.59	<b>0.0409</b>	1.72	0.1557
$X_1X_3$	1.37	0.4806	2.39	0.0630
$X_2X_3$	3.54	0.0949	0.98	0.3937
$X_1^2$	–4.41	<b>0.0429</b>	–22.70	<b>&lt;0.0001</b>
$X_2^2$	33.25	<b>&lt;0.0001</b>	3.05	<b>0.0230</b>
$X_3^2$	5.50	<b>0.0179</b>	–4.92	<b>0.0023</b>

<sup>a</sup> Values in boldface represented significant terms ( $p < 0.05$ ).

The LC–MS/MS method was fully validated according to the FDA guidelines for the validation of bioanalytical methods (USFDA, 2001). Good linearity was obtained over the concentration range of 1.0–1000.0 ng/mL ( $R^2 > 0.99$ ) and the lowest limit of quantification (LLOQ) for AG in rat plasma was 1.0 ng/mL. The intra- and inter-day precisions (RSD) of the QC samples at three concentration levels were less than 6.84% and 7.22%, respectively, while the accuracy was in the range of 98.3–106.6%. All the recoveries of the QC samples ranged from 78.6% to 95.1% and the matrix effects were between 101.4% and 106.2%. AG was found stable in plasma under all three stability test conditions. The accuracy values for AG in plasma at the low (5.0 ng/mL) and high (500.0 ng/mL) levels were 96.4 and 101.7% after 12 h at room temperature, 104.3 and 98.2% after three freeze–thaw cycles, and 105.6 and 102.8% at  $-20^\circ\text{C}$  for 3 weeks, respectively. The RSD values for AG in all the stability studies were within 1.29–8.13%. These results indicated that this assay could be applied for the quantification of AG in rat plasma.

### 2.7.3. Pharmacokinetic data analysis

The plasma concentration–time data were analyzed with compartmental model by DAS 2.1 software (Mathematical Pharmacology Professional Committee of China, Shanghai, China) to obtain the pharmacokinetic parameters, including area under the plasma concentration–time curve (AUC), half-life ( $t_{1/2}$ ), elimination rate constant ( $k$ ), and mean residence time (MRT). The maximum plasma drug concentration ( $C_{\text{max}}$ ) and the time required to reach  $C_{\text{max}}$  ( $t_{\text{max}}$ ) were directly read from the plasma concentration–time data. The absolute bioavailability ( $F$ ) was calculated as the ratio of  $(\text{AUC}/\text{dose})_{\text{im}}$  to  $(\text{AUC}/\text{dose})_{\text{iv}}$ .

## 2.8. In vitro–in vivo correlation (IVIVC) analysis

IVIVC of the AG loaded PLGA microspheres was evaluated by plotting the percent absorbed *in vivo* ( $F_a$ ) versus percent released *in vitro* ( $Q$ ). The percent released *in vitro* were taken from *in vitro* release data, and the Loo–Riegelman method was employed to



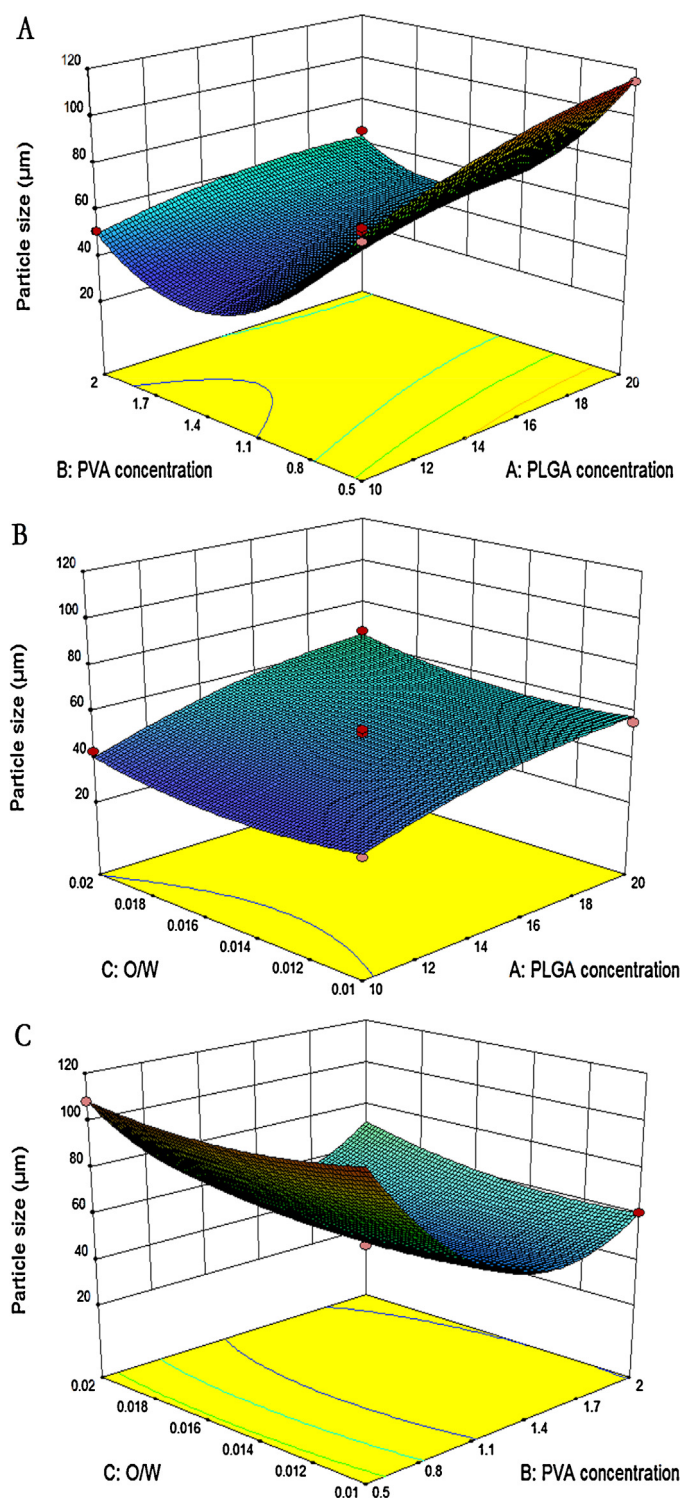


**Fig. 1.** Response surface plots showing the effects of (A) PLGA concentration ( $X_1$ ) and PVA concentration ( $X_2$ ); (B) PLGA concentration ( $X_1$ ) and o/w ratio ( $X_3$ ); (C) PVA concentration ( $X_2$ ) and o/w ratio ( $X_3$ ) on particle size ( $Y_1$ ).

calculate the fraction of drug absorbed *in vivo* from the plasma concentration data (Shargel et al., 2005).

$$F_a = \frac{(X_A)_t}{(X_A)_\infty} = \frac{C_p + C_t + k_{10}(AUC)_0^t}{k_{10}(AUC)_0^\infty} \quad (8)$$

where  $F_a$  is the fraction of drug absorbed,  $C_p$  is the drug concentration in central compartment (plasma),  $C_t$  is the apparent tissue compartment concentration,  $k_{10}$  is the elimination rate

constant,  $AUC_{0-\infty}$  or  $AUC_{0-t}$  is area under the plasma concentration–time curve from zero to infinity or time  $t$ . Linear regression analysis was applied to fit the IVIVC plot and the coefficient of determination ( $R^2$ ) was calculated to evaluate the IVIVC.

### 3. Results and discussion

#### 3.1. Preparation of the microspheres

The AG loaded PLGA microspheres have been successfully prepared by a *s/o/w* emulsion solvent evaporation method. In contrast to *w/o/w* emulsion method, *s/o/w* technique could produce the microspheres with relatively high drug loading capacity, and it has been used successfully to fabricate microspheres encapsulating various hydrophobic drugs (Liu et al., 2009). Taking into account of the requirement of getting high drug loading and the fact that AG has very poor aqueous solubility ( $\sim 0.05$  mg/mL) and limited solubility in organic solvents ( $< 2.5$  mg/mL in methylene chloride) (Chen and Wang, 2010), the AG loaded PLGA microspheres were prepared by a *s/o/w* emulsion method.

It is well known that the type of PLGA is one of the most important factor that can significantly influence the properties of the resultant microspheres (Mao et al., 2012; Tamber et al., 2005), thus it was firstly investigated in our preliminary experiments. As a result, the PLGA 5050 with Mw of 18 kDa was chosen for the present study based on the appropriate particle size, entrapment efficiency and drug release behavior.

As to drug substance, studies have shown that its crystal form and particle size have great effect on formation and properties of the resultant microspheres. It has been reported that an amorphous form of drug could give more homogenous *s/o* dispersion and thus more uniform distribution of drug throughout the microspheres, resulting in a lower initial burst release than its crystalline form (Takada et al., 1997). Moreover, particle size reduction for sparingly soluble drugs might increase powder surface areas and the volume ratio between microsphere and drug particle, which would improve the coating of drug particles in the polymer matrix during microsphere preparation and obtain a well-controlled release of drug (Geze et al., 1999). For these reasons, the drug substance of AG was subjected to wet grinding (DYNO-MILL<sup>®</sup> KDL, Willy A. Bachofen AG, Switzerland) and then freeze-drying to provide amorphous AG fine powder with a mean particle size of  $0.5 \mu\text{m}$  for the preparation of AG loaded PLGA microspheres in the present study.

#### 3.2. Statistical analysis of experimental data by Design-expert software

The response surface methodology (RSM) was used to identify the optimum levels of the process variables ( $X_1$ ,  $X_2$  and  $X_3$ ) which had significant effects on particle size ( $Y_1$ ) and entrapment efficiency ( $Y_2$ ). Based on the design matrix of BBD for three factors at three levels, a total of 17 experiments were then performed and the observed responses are summarized in Table 2.

All the responses observed for the 17 formulations prepared were fitted to various models using Design-Expert<sup>®</sup> software. It was observed that the best-fit model was the quadratic model for each response. The results of regression analysis for responses  $Y_1$  and  $Y_2$  are summarized in Table 3. Analysis of variance (ANOVA) was applied to estimate the significance of the quadratic models at the 5% significance level. The coefficients of the quadratic models and their corresponding  $p$ -values are shown in Table 4.

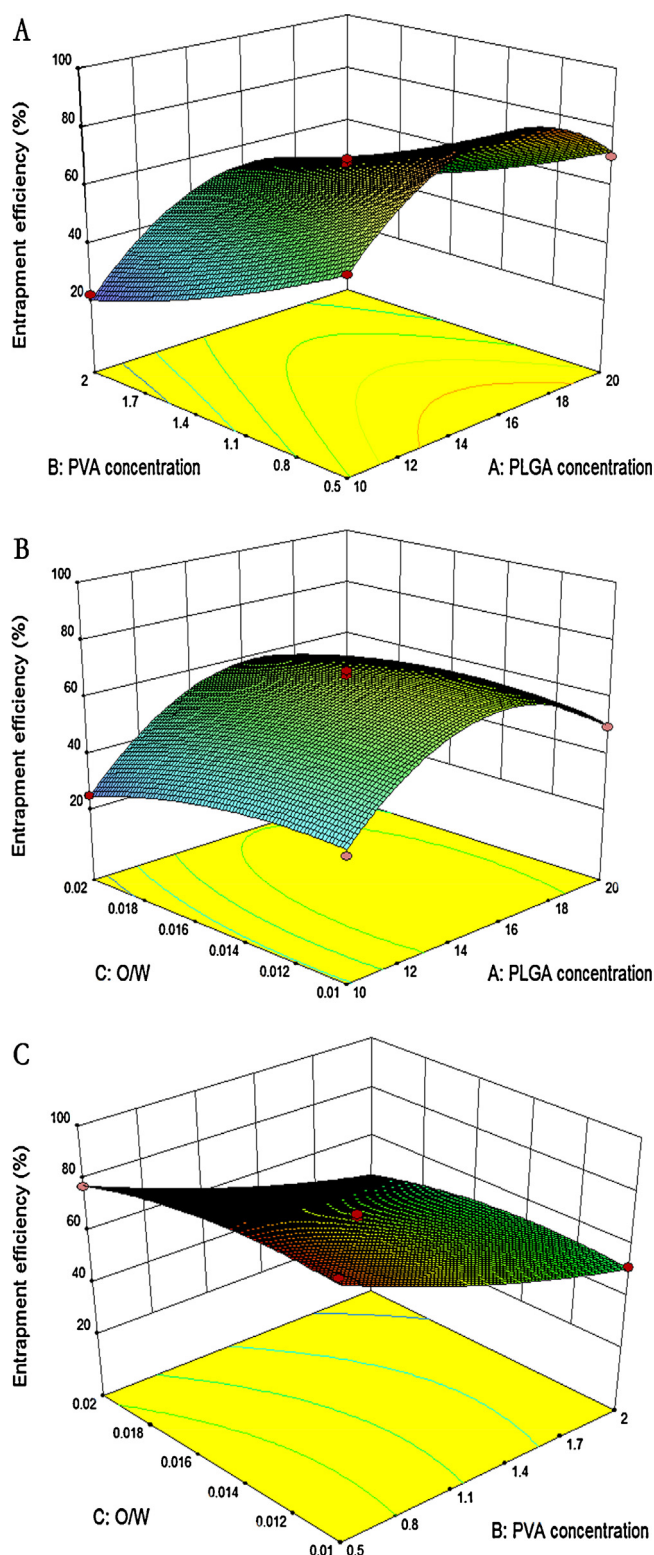


**Fig. 2.** Response surface plots showing the effects of (A) PLGA concentration ( $X_1$ ) and PVA concentration ( $X_2$ ); (B) PLGA concentration ( $X_1$ ) and o/w ratio ( $X_3$ ); (C) PVA concentration ( $X_2$ ) and o/w ratio ( $X_3$ ) on encapsulation efficiency ( $Y_2$ ).

The three-dimensional response surface plots generated by the regression models are shown in Figs. 1 and 2, which show the relationship between the independent variables and the responses graphically. The response surface plots were used to study the interaction effects of two factors on the response at a time, when the third factor is kept at constant level (Woitiski et al., 2009).

### 3.2.1. Effects on particle size ( $Y_1$ )

For response of  $Y_1$ , the experimental results were fitted into a second-order polynomial equation as following:

$$Y_1 = 49.54 + 11.18X_1 - 21.65X_2 + 2.19X_3 - 4.59X_1X_2 + 1.37X_1X_3 + 3.54X_2X_3 - 4.41X_1^2 + 33.25X_2^2 + 5.50X_3^2 \quad (9)$$

The model  $F$ -value of 81.19 implied that the model was significant ( $p < 0.0001$ ). The 'Lack of Fit  $F$ -value' of 2.42 implied that the Lack of Fit was not significant ( $p = 0.2063$ ). The  $R^2$  value of 0.9905 indicated a good correlation between the experimental and predicted values. The "Predicted  $R^2$ " of 0.8968 was in reasonable agreement with the "Adjusted  $R^2$ " of 0.9783, indicating the adequacy of the model to predict the response. "Adequate Precision" measures the signal to noise ratio. A ratio greater than 4 is desirable. The obtained ratio of 27.434 indicated an adequate signal. %CV of 5.58 represented the precision and reliability of the model. Therefore, this model could be used to navigate the design space.

The significance of each coefficient was determined by the  $p$ -value. The smaller the  $p$ -value, the more significant is the corresponding coefficient. Values of "Prob >  $F$ " less than 0.05 indicate the model terms are significant. As shown in Table 4,  $X_1$ ,  $X_2$ ,  $X_1X_2$ ,  $X_1^2$ ,  $X_2^2$  and  $X_3^2$  were significant model terms. A negative sign signifies antagonistic effect while a positive sign indicates a synergistic effect. It is thus evident that the PLGA concentration had a positive effect on particle size, while PVA concentration had a negative effect.

Fig. 1 is the response surface plot that shows the effect of the independent variables on particle size. The results showed that particle size increased significantly with increasing PLGA concentration. This could be explained by the fact that the viscosity of polymer solution increases with increasing polymer concentration (Mastiholmath et al., 2008), and a more viscous polymer solution is more difficult to be broken up into smaller droplets at the same input power of mixing (Yang et al., 2000). However, particle size was found to decrease markedly as PVA concentration increased. PVA acts as a droplet stabilizer and prevents coalescence of the droplets by localizing at the interface between the dispersed phase and dispersion medium (Mastiholmath et al., 2008).

### 3.2.2. Effects on entrapment efficiency ( $Y_2$ )

For response of  $Y_2$ , the experimental results were fitted into a second-order polynomial equation as following:

$$Y_2 = 67.49 + 8.35X_1 - 17.75X_2 - 4.43X_3 + 1.72X_1X_2 + 2.39X_1X_3 + 0.98X_2X_3 - 22.70X_1^2 + 3.05X_2^2 - 4.92X_3^2 \quad (10)$$

The model  $F$ -value of 133.33 implied that the model was significant ( $p < 0.0001$ ). The 'Lack of Fit  $F$ -value' of 3.60 implied that the Lack of Fit was not significant ( $p = 0.1239$ ). The  $R^2$  value of 0.9942 indicated a good fit. The "Predicted  $R^2$ " of 0.9298 was in reasonable agreement with the "Adjusted  $R^2$ " of 0.9867. The "Adequate Precision" of 41.461 indicated an adequate signal. %CV of 3.87 represented the precision and reliability of the model.

In this case,  $X_1$ ,  $X_2$ ,  $X_3$ ,  $X_1^2$ ,  $X_2^2$  and  $X_3^2$  were significant model terms. Positive coefficients of  $X_1$  and  $X_2^2$  in Eq. (10) indicated the synergistic effect on entrapment efficiency, while negative coefficients of  $X_2$ ,  $X_3$ ,  $X_1^2$  and  $X_3^2$  indicated the antagonistic effect.

As shown in Fig. 2, entrapment efficiency increased significantly as PLGA concentration increased. This could be attributed to the fact that the increased PLGA concentration would increase the viscosity of the medium and resulted in faster solidification, which would further prevent the diffusion of drug from inner phase to external phase (Rahman et al., 2010). However, entrapment efficiency was found to decrease markedly with an increase in PVA concentration. Higher concentration of PVA would increase the partitioning of drug from inner phase to external phase. This

**Table 5**

Comparative levels of predicted and observed responses for three checkpoint formulations.

Formulation composition ( $X_1/X_2/X_3$ )	Response	Predicted value	Observed value (mean $\pm$ SD, $n = 3$ )	Prediction error (%)
15.11/1.12/0.013	$Y_1$	54.67	$56.38 \pm 2.23$	3.13
	$Y_2$	71.82	$75.16 \pm 2.89$	4.65
12.5/1.75/0.018	$Y_1$	49.02	$52.14 \pm 2.14$	6.37
	$Y_2$	41.84	$38.64 \pm 1.28$	–7.64
17.5/0.75/0.015	$Y_1$	84.76	$88.89 \pm 4.11$	4.87
	$Y_2$	78.60	$80.73 \pm 3.64$	2.71

increased partitioning might result from increased solubility of drug in the external phase (Rahman et al., 2010). Similarly, increasing the o/w ratio led to a decrease in entrapment efficiency, probably because the increased ratio of o/w favors partition of the drug in the aqueous phase to decrease entrapment efficiency (Guhagarkar et al., 2009).

### 3.3. Optimization and model validation

The particle size and entrapment efficiency are the 2 key physicochemical properties of microspheres. The entrapment efficiency is important for assessing the drug loading capacity of microspheres, and thus increasing encapsulation efficiency can reduce the loss of drug and help to extend the duration and dosage of treatment (Freiberg and Zhu, 2004). Therefore, maximum entrapment efficiency was chosen as one of the optimization criteria. In addition, the size of microspheres can affect the

syringeability and injectability of the product and the drug release rate (Mao et al., 2012). In this work, the average particle size of 17 experimental runs in the BBD ranged from  $37.11 \mu\text{m}$  to  $115.09 \mu\text{m}$ , so we selected minimum particle size as one of optimization criteria in order to make the microspheres suitable for administration via i.m. injection.

A numerical optimization technique by the desirability function using Design-Expert software was used to obtain the optimum values of the independent variables. The optimum formulation was selected based on the set criteria of minimum particle size and maximum entrapment efficiency. Finally, the optimized formulation was achieved with 15.11% PLGA concentration (w/v), 1.12% PVA concentration (w/v) and 0.013 o/w ratio (v/v), respectively. These values predict particle size of  $54.67 \mu\text{m}$  and entrapment efficiency of 71.82%.

To confirm the validity of the model generated by the software, three checkpoint formulations including two random checkpoints and the optimum levels of independent variables were prepared. The composition of checkpoint formulations, the predicted and observed values for the responses and the prediction error (%) are shown in Table 5. The low value of prediction error (below 15%) indicated that the observed responses were in close agreement with the predicted values and that the model was valid. It can also be concluded that the optimization technique was appropriate for optimizing the AG loaded PLGA microspheres. Thereafter, all of the following experiments were conducted using the microspheres produced by the optimized formulation.

### 3.4. Characterization of AG loaded microspheres

The surface morphology of AG loaded PLGA microspheres observed by the scanning electron microscopy (SEM) is shown in Fig. 3A, which revealed that the microspheres were spherical in shape with a smooth surface.

As shown in Fig. 3B, the mean particle size of the microspheres was  $53.18 \pm 2.11 \mu\text{m}$  and the PDI was 0.216, indicating a rather narrow particle size distribution. Such particle size and narrow size distribution are considered to be suitable for i.m. injection.

The entrapment efficiency and drug loading of the AG loaded microspheres prepared with optimized formulation were determined to be  $75.79 \pm 3.02\%$  and  $47.06 \pm 2.18\%$ , respectively. Moreover, encapsulation of AG into PLGA microspheres with such a high drug loading may overcome the defects of conventional oral dosage forms of AG (tablets and dripping pills), which include low bioavailability and frequent administration.

### 3.5. Residual solvent analysis

Due to the high tissue toxicity, removal of organic solvents during microspheres manufacturing is critical, and it is therefore an industrial requirement to confine organic solvents residue within their acceptable levels (Mathew et al., 2013). Solvent used in the preparation of AG loaded PLGA microspheres was methylene chloride. By GC analysis, the maximum residual content of

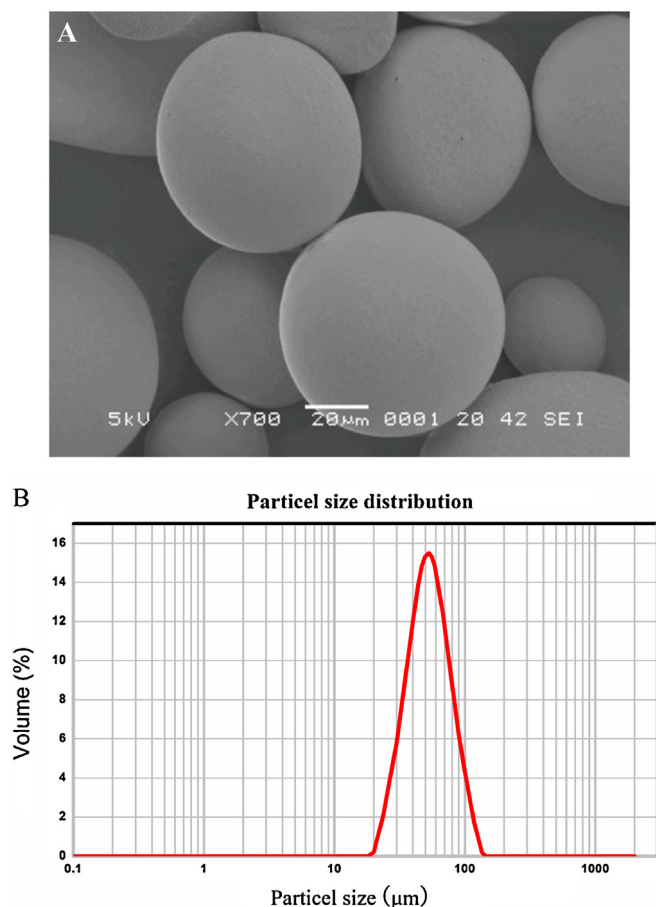


**Fig. 3.** SEM image ( $\times 700$ ) (A) and particle size distribution (B) of AG loaded PLGA microspheres.



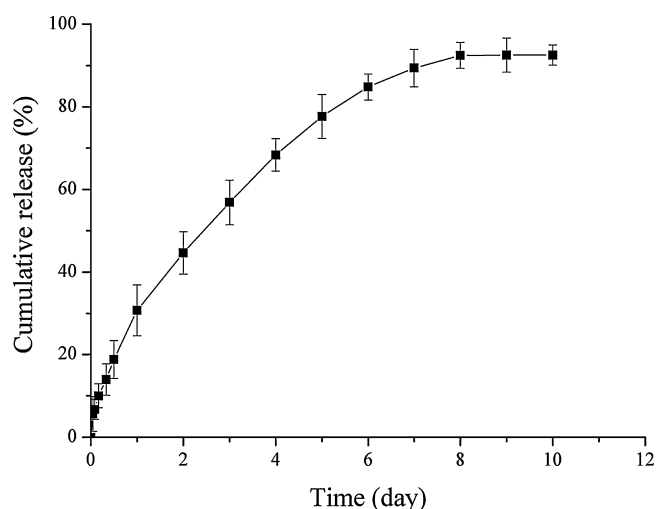


**Fig. 4.** *In vitro* release profile of AG loaded PLGA microspheres. Each point represents mean  $\pm$  SD ( $n=3$ ).

methylene chloride in the microspheres was determined as  $38.5 \pm 1.4$  ppm and satisfied the requirements of ICH, which provide that methylene chloride is a Class 2 organic solvent and its concentration limit (ppm) and PDE (permitted daily exposure) are 600 ppm and 6.0 mg/day, respectively (ICH, 2009). The result demonstrated very limited toxic residues and the effectiveness of stirring process to eliminate organic solvent in the microspheres.

### 3.6. *In vitro* drug release

The cumulative release profile of AG from the PLGA microspheres in PBS is shown in Fig. 4. The result displayed a sustained release of AG from the PLGA microspheres up to 9 days after a low initial burst release of approximately 14% within the first 8 h. The initial burst release could be explained by drug desorption from the outer surface of the drug delivery system (Nath et al., 2013). Therefore, the low initial burst release suggested lower AG density at the surface of the PLGA microspheres.

The mechanism of AG release from the PLGA microspheres was investigated by fitting the data obtained from *in vitro* release study into zero order, first order, Higuchi and Korsmeyer–Peppas models. The coefficient of determination ( $R^2$ ), release rate constant ( $k$ ) and  $n$  values obtained after linear regression on various kinetic models are shown in Table 6. It was found that the *in vitro* release data was followed and supported by the Korsmeyer–Peppas model as it presented the highest value of  $R^2$  (0.9935). Moreover, the value of  $n$  was 0.5663, suggesting a non-Fickian diffusion kinetics ( $0.5 < n < 1$ ) (Peppas, 1985). Hence, it is concluded that the drug release mechanism was mainly due to the combination of diffusion of drug through the polymeric matrix and polymer erosion of the PLGA microspheres (Erdemli et al., 2014).

**Table 6**

The kinetic models simulated for the release behavior of AG loaded PLGA microspheres.

Model	Equation	$R^2$
Zero-order model	$y = 0.004x + 0.1687$	0.9087
First-order model	$y = -0.0119x - 0.0646$	0.9847
Higuchi model	$y = 0.0676x - 0.0207$	0.9858
Korsmeyer–Peppas model	$y = 0.5598x - 3.0109$	0.9935

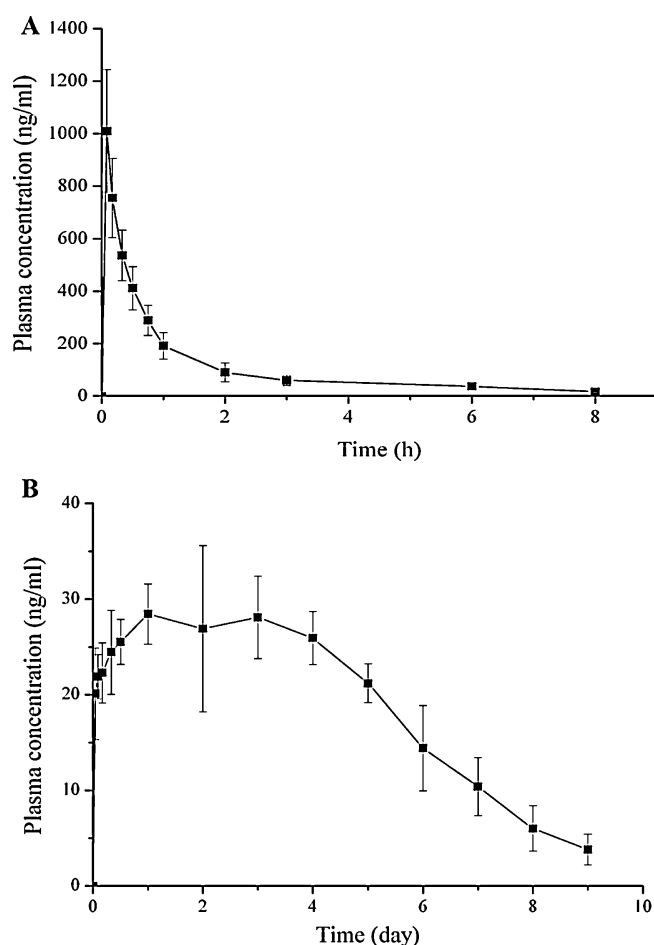


**Fig. 5.** Mean plasma concentration–time profiles of AG in rats following (A) i.v. administration of pure AG solution at a single dose of 2 mg/kg and (B) i.m. administration of AG loaded PLGA microspheres at a single dose of 10 mg/kg (mean  $\pm$  SD,  $n=6$ ).

### 3.7. *In vivo* pharmacokinetic study

The mean plasma concentration–time profiles of AG in rats after i.v. administration of pure AG solution and i.m. administration of AG loaded PLGA microspheres are shown in Fig. 5. The results demonstrated that the concentration–time curves of both pure AG solution and AG loaded PLGA microspheres could be fitted to the two-compartment model and the main pharmacokinetic parameters calculated for AG are listed in Table 7.

In the case of the microspheres, the plasma concentration of AG attained  $C_{\max}$  of  $28.44 \pm 3.76$  ng/mL at  $t_{\max}$  of  $23.73 \pm 2.25$  h. In addition, the  $t_{1/2\alpha}$  and  $t_{1/2\beta}$  of the microspheres were  $24.84 \pm 3.01$  h and  $36.27 \pm 5.16$  h, respectively, suggesting a rather

**Table 7**

Pharmacokinetic parameters of AG in rats following i.v. administration of pure AG solution at a single dose of 2 mg/kg and i.m. administration of AG loaded PLGA microspheres at a single dose of 10 mg/kg (mean  $\pm$  SD,  $n=6$ ).

Parameter	AG solution	AG loaded PLGA Microspheres
$t_{1/2\alpha}$ (h)	$0.054 \pm 0.008$	$24.84 \pm 3.01$
$t_{1/2\beta}$ (h)	$0.57 \pm 0.11$	$36.27 \pm 5.16$
$AUC_{0-\infty}$ (ng h/mL)	$1294.8 \pm 250.3$	$4370.6 \pm 613.8$
MRT (h)	$2.42 \pm 0.19$	$91.68 \pm 10.94$
$k_{10}$ ( $h^{-1}$ )	$2.38 \pm 0.13$	$0.08 \pm 0.02$
$k_{12}$ ( $h^{-1}$ )	$6.342 \pm 0.452$	$0.057 \pm 0.014$
$k_{21}$ ( $h^{-1}$ )	$5.287 \pm 0.297$	$0.024 \pm 0.007$
$F$ (%)	–	67.51



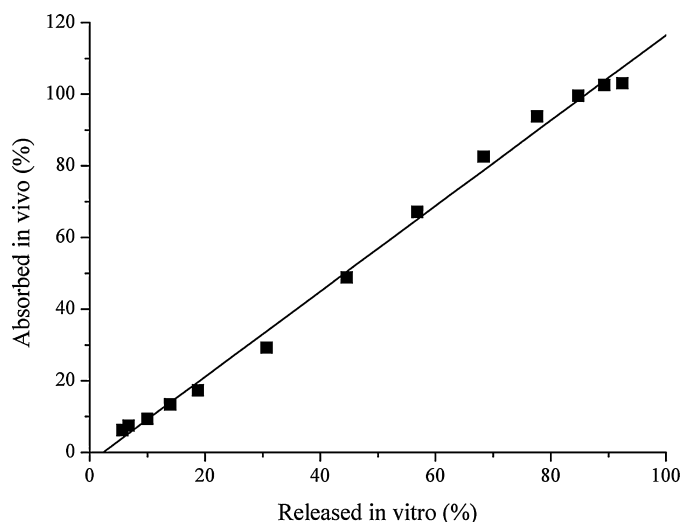


Fig. 6. Linear regression plot of percent absorbed *in vivo* versus percent released *in vitro*.

slow *in vivo* distribution and elimination. The MRT value of the microspheres was  $91.68 \pm 10.94$  h and nearly 40-fold longer than that of pure AG solution, which further indicated obvious sustainable release properties of the microspheres. Moreover, the AUC values were  $1294.8 \pm 250.3$  ng h/mL and  $4370.6 \pm 613.8$  ng h/mL for pure AG solution and the microspheres, respectively. Consequently, the absolute bioavailability of the microspheres was calculated as 67.51%, which demonstrated a relatively high and effective absorption of AG *in vivo* after i.m. administration of AG loaded PLGA microspheres.

### 3.8. In vitro–in vivo correlation (IVIVC)

The *in vitro* and *in vivo* correlation is always a crucial issue for the dosage forms in which the drug needs to be absorbed into circulation, since it is important for both formulation development and quality control (Sun et al., 2008). In this study, a point-to-point relationship between *in vitro* drug release and *in vivo* drug absorption was observed for AG loaded PLGA microspheres. The point-to-point relationship was classified as level A correlation by the US Food and Drug Administration (Dressman and Reppas, 2000).

The fraction of AG absorbed *in vivo* was determined by deconvolution using Loo–Riegelman method since the pharmacokinetics of AG was fitted to a 2 compartmental model. The IVIVC of the microspheres was illustrated by the linear regression plot of percent absorbed *in vivo* versus percent released *in vitro* (Fig. 6). A good linear relationship for the microspheres was observed between the fraction of AG absorbed *in vivo* and the percent released *in vitro*:  $y = 1.1916x - 2.708$  ( $R^2 = 0.9951$ ). Therefore, the results indicated that the AG loaded PLGA microspheres presented a similar release profile *in vitro* and *in vivo*, moreover, it seemed to be reasonable to predict the drug absorption *in vivo* through the *in vitro* release study.

## 4. Conclusions

In the present study, the injectable PLGA microspheres were used to develop a sustained-release delivery system of AG to improve the potential utility for cancer chemotherapy. A s/o/w emulsion solvent evaporation method was used for microspheres fabrication and RSM method was applied for formulation design and optimization. Consequently, the AG loaded PLGA microspheres were obtained with relatively high entrapment efficiency and

small particle size. Both *in vitro* and *in vivo* experiments demonstrated sustained release of AG from the PLGA microspheres. Moreover, a good linear correlation between *in vitro* and *in vivo* release was obtained, suggesting that the *in vitro* release technique was suitable for both quality control purposes and *in vivo* performance prediction of the PLGA microspheres. Therefore, these results suggest that the PLGA microspheres might be a promising formulation for AG used for cancer therapy.

## Acknowledgments

This work was supported by the National Key Technology Research and Development Program (No. 2012BAK25B03-3) and the Youth Scholar Backbone Training Plan Project of Yantai University (2012–2016).

## References

- Akbar, S., 2011. *Andrographis paniculata*: a review of pharmacological activities and clinical effects. *Altern. Med. Rev.* 16, 66–77.
- Barrow, W.W., 2004. Microsphere technology for chemotherapy of mycobacterial infections. *Curr. Pharm. Des.* 10, 3275–3284.
- Benoit, J.P., Faisant, N., Menei, P., 2000. Use of biodegradable microspheres for the delivery of an anticancer agent for the treatment of glioblastoma. EP20000401344.
- Boik, J., 2001. *Natural Compounds in Cancer Therapy*. Oregon Medical Press, Minnesota, USA.
- Bothiraja, C., Shinde, M.B., Rajalakshmi, S., Pawar, A.P., 2009. Evaluation of molecular pharmaceutical and *in-vivo* properties of spray-dried isolated andrographolide-PVP. *J. Pharm. Pharmacol.* 61, 1465–1472.
- Chellampillai, B., Pawar, A.P., 2011. Improved bioavailability of orally administered andrographolide from pH-sensitive nanoparticles. *Eur. J. Drug Metabol. Pharmacokinet.* 35, 123–129.
- Chen, L.L., Wang, Z.H., 2010. Investigation of basic physical and chemical properties of andrographolide. *Pharm. Today* 1, 015.
- Cheung, R.Y., Ying, Y., Rauth, A.M., Marcon, N., Yu Wu, X., 2005. Biodegradable dextran-based microspheres for delivery of anticancer drug mitomycin C. *Biomaterials* 26, 5375–5385.
- Cragg, G.M., Newman, D.J., 2005. Plants as a source of anti-cancer agents. *J. Ethnopharmacol.* 100, 72–79.
- Deng, W.L., 1978. Outline of current clinical and pharmacological research on *Andrographis paniculata* in China. *Newslett. Chin. Herb. Med.* 10, 27–31.
- Dressman, J.B., Reppas, C., 2000. *In vitro–in vivo* correlations for lipophilic, poorly water-soluble drugs. *Eur. J. Pharm. Sci.* 11, S73–S80.
- Efferth, T., Li, P.C.H., Konkimala, V.S.B., Kaina, B., 2007. From traditional Chinese medicine to rational cancer therapy. *Trends Mol. Med.* 13, 353–361.
- Erdemli, Usanmaz, A., Keskin, D., Tezcaner, A., 2014. Characteristics and release profiles of MPEG–PCL–MPEG microspheres containing immunoglobulin G. *Colloids Surf. B: Biointerfaces* 117, 487–496.
- Freiberg, S., Zhu, X.X., 2004. Polymer microspheres for controlled drug release. *Int. J. Pharm.* 282, 1–18.
- Gannu, R., Palem, C.R., Yamsani, V.V., Yamsani, S.K., Yamsani, M.R., 2010. Enhanced bioavailability of lacidipine via microemulsion based transdermal gels: formulation optimization, *ex vivo* and *in vivo* characterization. *Int. J. Pharm.* 388, 231–241.
- Geze, A., Venier-Julienne, M.C., Mathieu, D., Filmon, R., Phan-Tan-Luu, R., Benoit, J.P., 1999. Development of 5-iodo-2'-deoxyuridine milling process to reduce initial burst release from PLGA microparticles. *Int. J. Pharm.* 178, 257–268.
- Gu, Y., Ma, J., Liu, Y., Chen, B., Yao, S., 2007. Determination of andrographolide in human plasma by high-performance liquid chromatography/mass spectrometry. *J. Chromatogr. B* 854, 328–331.
- Guhagarkar, S.A., Maishe, V.C., Devarajan, P.V., 2009. Nanoparticles of polyethylene sebacate: a new biodegradable polymer. *AAPS PharmSciTech* 10, 935–942.
- Higuchi, T., 1963. Mechanism of sustained action medication, theoretical analysis of rate of release of solid drugs dispersed in solid matrices. *J. Pharm. Sci.* 52, 1145–1149.
- Hu, Z.H., Wang, Q.J., Liao, M.Y., 2009. Nephrotoxicity of andrographolide injection and its safe use. *Adv. Drug React. J.* 1, 013.
- ICH, 2009. Harmonised Tripartite Guideline. Impurities: Guideline for Residual Solvents, Q3C (R4). ICH, Geneva, Switzerland.
- Korsmeyer, R.W., Gurny, R., Doelker, E., Buri, P., Peppas, N.A., 1983. Mechanisms of solute release from porous hydrophilic polymers. *Int. J. Pharm.* 15, 25–35.
- Kumar, R.A., Sridevi, K., Kumar, N.V., Nanduri, S., Rajagopal, S., 2004. Anticancer and immunostimulatory compounds from *Andrographis paniculata*. *J. Ethnopharmacol.* 92, 291–295.
- Liu, L.B., Zhang, Y.Q., Guo, S.R., 2009. Preparation and *in vitro* release behavior of 5-fluorouracil loaded sustained release microspheres by S/O/W method. *Chin. Pharm. J.* 44, 205–208.
- Liu, Z., Ballinger, J.R., Rauth, A.M., Bendayan, R., Wu, X.Y., 2003. Delivery of an anticancer drug and a chemosensitizer to murine breast sarcoma by

- intratumoral injection of sulfopropyl dextran microspheres. *J. Pharm. Pharmacol.* 55, 1063–1073.
- Lu, H., Zhang, X.Y., Zhou, Y.Q., Jin, S.S., 2010. Toxic actions of andrographolide sodium bisulfite on kidneys of mice and rabbits. *Chin. J. Pharmacol. Toxicol.* 3, 012.
- Maiti, K., Gantait, A., Mukherjee, K., Saha, B.P., Mukherjee, P.K., 2006. Therapeutic potentials of andrographolide from *Andrographis paniculata*: a review. *J. Nat. Remedies* 6, 1–13.
- Mandal, S.C., Dhara, A.K., Maiti, B.C., 2001. Studies on psychopharmacological activity of *Andrographis paniculata* extract. *Phytother. Res.* 15, 253–256.
- Mao, S., Guo, C., Shi, Y., Li, L.C., 2012. Recent advances in polymeric microspheres for parenteral drug delivery – part 1. *Expert Opin. Drug Deliv.* 9, 1161–1176.
- Mastiholmath, V.S., Dandagi, P.M., Gadad, A.P., Mathews, R., Kulkarni, A.R., 2008. In vitro and in vivo evaluation of ranitidine hydrochloride ethyl cellulose floating microparticles. *J. Microencapsul.* 25, 307–314.
- Mathew, S.T., Subbiah, G.D., Vasanth, P.V., Balan, V., 2013. Characterization and pharmacokinetic evaluation of gamma sterilized ketorolac tromethamine loaded albumin microspheres for intramuscular administration. *Curr. Drug Deliv.* 10, 158–166.
- Nath, S.D., Son, S., Sadiasa, A., Min, Y.K., Lee, B.T., 2013. Preparation and characterization of PLGA microspheres by the electrospraying method for delivering simvastatin for bone regeneration. *Int. J. Pharm.* 443, 87–94.
- Newman, D.J., Cragg, G.M., 2012. Natural products as sources of new drugs over the 30 years from 1981 to 2010. *J. Nat. Products* 75, 311–335.
- Panossian, A., Hovhannissyan, A., Mamikonyan, G., Abrahamian, H., Hambardzumyan, E., Gabrielian, E., Goukasova, G., Wikman, G., Wagner, H., 2000. Pharmacokinetic and oral bioavailability of andrographolide from *Andrographis paniculata* fixed combination Kan Jang in rats and human. *Phytomedicine* 7, 351–364.
- Peppas, N.A., 1985. Analysis of Fickian and non-Fickian drug release from polymers. *Pharm. Acta Helvetiae* 60, 110–111.
- Rahman, Z., Zidan, A.S., Habib, M.J., Khan, M.A., 2010. Understanding the quality of protein loaded PLGA nanoparticles variability by Plackett–Burman design. *Int. J. Pharm.* 389, 186–194.
- Rajagopal, S., Kumar, R.A., Deevi, D.S., Satyanarayana, C., Rajagopalan, R., 2003. Andrographolide, a potential cancer therapeutic agent isolated from *Andrographis paniculata*. *J. Exp. Ther. Oncol.* 3, 147–158.
- Roy, P., Das, S., Bera, T., Mondol, S., Mukherjee, A., 2009. Andrographolide nanoparticles in leishmaniasis: characterization and *in vitro* evaluations. *Int. J. Nanomed.* 5, 1113–1121.
- Shargel, L., Yu, A.B.C., Wu-Pong, S., 2005. Pharmacokinetics of oral absorption, In: Shargel, L., Yu, A.B.C., Wu-Pong, S. (Eds.), *Applied Biopharmaceutics and Pharmacokinetics*. 5th ed. The McGraw Hill, 161–184.
- Sinha, J., Mukhopadhyay, S., Das, N., Basu, M.K., 2000. Targeting of liposomal andrographolide to L. donovani-infected macrophages *in vivo*. *Drug Deliv.* 7, 209–213.
- Sinha, V.R., Trehan, A., 2005. Biodegradable microspheres for parenteral delivery. *Crit. Rev. Ther. Drug Carrier Syst.* 22, 535–602.
- Sudhakaran, M.V., 2012. Botanical pharmacognosy of *Andrographis paniculata* (Burm F.) Wall. Ex. Nees. *Phcog. J.* 4, 1–10.
- Sun, Y., Wang, J., Zhang, X., Zhang, Z., Zheng, Y., Chen, D., Zhang, Q., 2008. Synchronic release of two hormonal contraceptives for about one month from the PLGA microspheres: *in vitro* and *in vivo* studies. *J. Control. Release* 129, 192–199.
- Takada, S., Kurokawa, T., Miyazaki, K., Iwasa, S., Ogawa, Y., 1997. Utilization of an amorphous form of water-soluble GP II b/IIIa antagonist for controlled release from biodegradable microspheres. *Pharm. Res.* 14, 1146–1150.
- Tamber, H., Johansen, P., Merkle, H.P., Gander, B., 2005. Formulation aspects of biodegradable polymeric microspheres for antigen delivery. *Adv. Drug Deliv. Rev.* 57, 357–376.
- Tang, W., Eisenbrand, G., 1992. *Chinese Drugs of Plant Origin*. Springer, Berlin.
- Toyama, T., Nitta, N., Ohta, S., Tanaka, T., Nagatani, Y., Takahashi, M., Murata, K., Shiomi, H., Naka, S., Kurumi, Y., Tani, T., Tabata, Y., 2012. Clinical trial of cisplatin-conjugated gelatin microspheres for patients with hepatocellular carcinoma. *Jpn. J. Radiol.* 30, 62–68.
- USFDA, 2001. <http://www.fda.gov/downloads/Drug/GuidanceComplianceRegulatoryInformation/Guidances/ucm070107.pdf>.
- Varma, A., Padh, H., Shrivastava, N., 2011. Andrographolide: a new plant-derived antineoplastic entity on horizon. *Evid. Based Complement. Alternat. Med.* 1–9.
- Ventura, C.A., Cannavà, C., Stancanelli, R., Paolino, D., Cosco, D., La Mantia, A., Pignatello, R., Tommasini, S., 2011. Gemcitabine-loaded chitosan microspheres. Characterization and biological *in vitro* evaluation. *Biomed. Microdevices* 13, 799–807.
- Vojdani, A., Erde, J., 2006. Regulatory T cells, a potent immunoregulatory target for CAM researchers: modulating tumor immunity, autoimmunity and alloreactive immunity (III). *Evid. Based Complement. Alternat. Med.* 3, 309–316.
- Wang, Y.M., Sato, H., Adachi, I., Horikoshi, I., 1996. Preparation and characterization of poly (lactic-co-glycolic acid) microspheres for targeted delivery of a novel anticancer agent, taxol. *Chem. Pharm. Bull.* 44, 1935–1940.
- Woitiski, C.B., Veiga, F., Ribeiro, A., Neufeld, R., 2009. Design for optimization of nanoparticles integrating biomaterials for orally dosed insulin. *Eur. J. Pharm. Biopharm.* 73, 25–33.
- Xu, L., Xiao, D.W., Lou, S., Zou, J.J., Zhu, Y.B., Fan, H.W., Wang, G.J., 2009. A simple and sensitive HPLC–ESI–MS/MS method for the determination of andrographolide in human plasma. *J. Chromatogr. B* 877, 502–506.
- Yang, C.R., Zhao, X.L., Hu, H.Y., Li, K.X., Sun, X., Li, L., Chen, D.W., 2010. Preparation, optimization and characteristic of huperzine A loaded nanostructured lipid carriers. *Chem. Pharm. Bull.* 58, 656–661.
- Yang, Y.Y., Chung, T.S., Bai, X.L., Chan, W.K., 2000. Effect of preparation conditions on morphology and release profiles of biodegradable polymeric microspheres containing protein fabricated by double-emulsion method. *Chem. Eng. Sci.* 55, 2223–2236.
- Ye, L., Wang, T., Tang, L., Liu, W., Yang, Z., Zhou, J., Zheng, Z., Cai, Z., Hu, M., Liu, Z., 2011. Poor oral bioavailability of a promising anticancer agent andrographolide is due to extensive metabolism and efflux by P-glycoprotein. *J. Pharm. Sci.* 100, 5007–5017.
- Zhao, D., Liao, K., Ma, X., Yan, X., 2002. Study of the supramolecular inclusion of  $\beta$ -cyclodextrin with andrographolide. *J. Incl. Phenom. Macrocycl. Chem.* 43, 259–264.